

ParaVT: Taming the Tool Prior Paradox for Parallel Tool Use in Agentic Video Reinforcement Learning

Zuhao Yang^{2,6,♡} Kaichen Zhang^{3,6,♡} Sudong Wang^{4,♡} Keming Wu^{5,6,♡} Zhongyu Yang²
 Bo Li⁶ Xiaojuan Qi³ Shijian Lu^{2,∞} Xingxuan Li^{1,∞} Lidong Bing¹

¹MiroMind ²NTU ³HKU ⁴HKUST(GZ) ⁵THU ⁶LMMs-Lab

<https://evolvinglmm-lab.github.io/ParaVT/>

Abstract

Training large multimodal models (LMMs) via reinforcement learning (RL) to natively invoke video-processing tools (*e.g.*, cropping) has become a promising route to long-video understanding. However, existing native-RL methods dispatch tool calls sequentially (*i.e.*, one per turn): a single wrong crop propagates errors without peer correction, multi-turn tool calls corrupt context, and inference cost scales linearly with the number of turns. We introduce **ParaVT**, the first multi-agent end-to-end RL-trained framework for **Parallel Video Tool** calling, dispatching multiple time-window crops in a single turn for cleaner context and better fault tolerance. Yet applying standard RL to ParaVT reveals an obstacle we term the *Tool Prior Paradox*: the pretrained tool priors that enable tool exploration also destabilize cold-started structural format and expose the skip-tool reward shortcut under temperature sampling. A cross-model contrast on a weaker-prior LMM supports this claim: format stays stable but RL elicits zero tool calls, indicating that prior strength is the shared driver of both format collapse and tool exploration. We propose **PARA-GRPO** (Parseability-Anchored and Ratio-gAteD **GRPO**), which augments standard RL with two complementary mechanisms: (i) a *targeted format reward* applied only at the structural-token positions most prone to collapse, and (ii) a *per-prompt frame-budget randomization* that creates training prompts where calling the tool yields a measurable reward signal over skipping it. Across six long-video understanding benchmarks, ParaVT improves over the Qwen3-VL baseline by +7.9% on average, with PARA-GRPO lifting training-time format compliance from 0.13 to 0.64. As tool capabilities become increasingly internalized in modern LMMs, RL must cooperate with the resulting priors, and ParaVT offers a general recipe for agentic RL. Our code, data, and model weights are publicly available at <https://github.com/EvolvingLMMs-Lab/ParaVT>.

1 Introduction

Recently, long-video understanding has been reframed as an *agentic video reasoning* problem. To answer “Which player took the decisive volley in this ninety-minute soccer match?”, a large multimodal model (LMM) is post-trained to invoke video-processing tools via supervised fine-tuning (SFT) on customized tool-use traces followed by reinforcement learning (RL) with verifiable rewards [6, 15, 21, 28, 41, 45, 47]. For example, LongVT [41] pairs SFT on *locate-and-inspect* chains-of-thought with multi-turn RL, instilling behaviors like skimming the match, zooming into the few seconds of evidence, and rewinding if the previous guess is wrong. These methods, however, all dispatch tool calls sequentially across turns (*i.e.*, one tool call per turn), with successive tool outputs accumulating in a single context window. This paradigm is brittle along three dimensions (Figure 3a): (i) a single mis-localized crop propagates errors with no peer to correct it; (ii) multi-turn accumulation aggregates context corruption; (iii) inference cost scales linearly with the number of turns.

To this end, we introduce **ParaVT**, the first multi-agent end-to-end RL-trained framework for **Parallel Video Tool** calling (Figure 3b). Within ParaVT, a main agent issues multiple temporal-window crops

♡ Work largely done during Z.Y., K.Z., S.W., and K.W.’s internship at MiroMind. ∞ Corresponding Author.

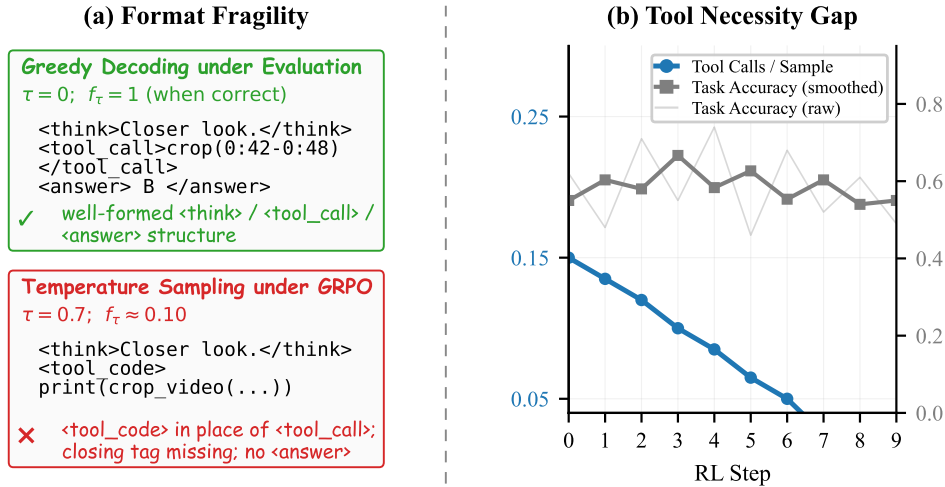


Figure 1: **Two Failure Modes of the Tool Prior Paradox.** (a) *Format Fragility*: rollouts are well-formed under greedy decoding (sampling temperature $\tau=0$, format reward ≈ 1); under temperature sampling within vanilla GRPO ($\tau=0.7$), the policy reverts to the pretrained `<tool_code>` tag in place of `<tool_call>`, often drops closing tags, and stops emitting `<answer>` altogether ($f_\tau \approx 0.1$). (b) *Tool Necessity Gap*: tool-call count drops to near-zero within 7 steps while task accuracy oscillates between 0.45 and 0.74, as the policy converges on the shortcut of skipping tools.

in a single turn, dispatches them to multiple sub-agents that work in parallel, and aggregates the evidence from each sub-agent for decision-making. Each sub-agent grounds an independent window, so the visual budget is re-allocated across peers and any single mis-localization can be outvoted.

A natural choice for end-to-end ParaVT training is Group Relative Policy Optimization (GRPO) [12] on top of a tool-native cold-started Qwen3-VL [1] checkpoint. However, vanilla GRPO exhibits two coupled training-time failures. The first is *Format Fragility* (Figure 1a): the SFT-learned `<think>/<tool_call>/<answer>` format is reliable under greedy decoding but, within a few vanilla-GRPO steps under temperature sampling, the policy reverts to the pretrained `<tool_code>` schema. This is a shallow override of the SFT format reminiscent of the Superficial Alignment Hypothesis [52], compounded by the competing *pretrained tool priors*: the probability mass on tool-call continuations carried over from pretraining (before SFT) that resurfaces under RL-time temperature. As a result, malformed rollouts cannot be parsed into rewardable tool calls, so the GRPO advantage signal is computed over a corrupted trajectory population before any tool-use credit can be assigned. The second is *Tool Necessity Gap* (Figure 1b): when uniformly-sampled overview frames suffice to answer many prompts directly, the reward gap between “call tool” and “skip tool” rollouts is near-zero, so GRPO’s group-normalized advantage on the call/skip dimension is also near-zero, and the policy converges to the canonical reward-hacking shortcut of skipping tools [29].

To probe the role of pretrained tool priors, we replicate the same setup on Qwen2.5-VL [25] (with much weaker tool priors than Qwen3-VL) under identical hyperparameters (Figure 2): its format stays near-perfect, yet RL elicits no tool calls. This cross-model contrast points to a paradoxical trade-off in prior strength: the pretrained tool priors are needed to elicit tool exploration, yet they

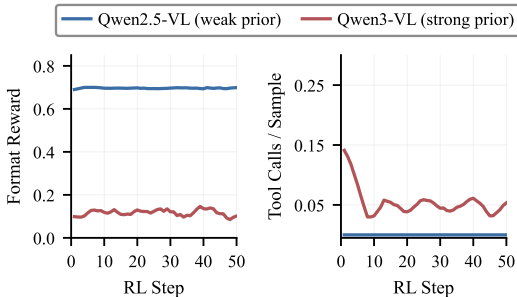


Figure 2: **Cross-Model Evidence for the Tool Prior Paradox under Vanilla GRPO.** Qwen3-VL-8B (stronger tool prior) explores tool use but collapses on format, while Qwen2.5-VL-7B (weaker tool prior) stays format-perfect yet emits zero tool calls.

destabilize the cold-started structural format and expose the skip-tool reward shortcut. Weakening the priors stabilizes format but cancels tool exploration altogether. We collectively term this trade-off the *Tool Prior Paradox*. This brings us to the central question of this work: *for tool-native LMMs, does the pretrained tool prior help or hurt tool use after RL?*

We propose **PARA-GRPO** (**P**arseability-**A**nchored and **R**atio-gAted **GRPO**) with *Exploration Anchoring* and *nFrames Gating* to tame the Tool Prior Paradox (Section 3.2). Exploration Anchoring stabilizes the format side via two cooperating mechanisms: a selective reward term targets the few structural-token positions most vulnerable to collapse, and a Constrained Generation hook fixes only the opening reasoning tag. Together they anchor rollout parseability without restricting reasoning content or tool-call sequences. nFrames Gating tackles the reward-signal side: randomizing the overview-frame budget per prompt creates a curriculum where a fraction of prompts cannot be answered from overview frames alone, gating a non-trivial call/skip advantage ratio that vanilla GRPO would otherwise average to zero. The two design choices are complementary: anchoring keeps rollouts well-formed enough to be parseable, and only on parseable rollouts can gating credit the tool-reward gradient. Empirically, PARA-GRPO lifts training-time format reward from 0.13 to 0.64 and improves the agentic-setting Qwen3-VL baseline on every tested benchmark (Section 4.2).

Our contributions are four-fold. **(i)** We introduce ParaVT, to our knowledge, the first framework that post-trains a tool-native LMM for parallel multi-tool calling in long-video understanding via agentic RL. ParaVT is trained on self-curated data: a 97K-sample multi-task SFT split (e.g., general video QA, parallel-tool traces, and long-video reasoning), followed by a separate 4.4K-sample RL split covering open-ended QA, multiple-choice, and temporal grounding. *Code, data, and model weights are publicly available.* **(ii)** We identify the Tool Prior Paradox, decompose it into Format Fragility and Tool Necessity Gap, and verify the diagnosis with a cross-model contrast on a weak-prior LMM. **(iii)** We propose PARA-GRPO, which introduces Exploration Anchoring and nFrames Gating to tackle Format Fragility and Tool Necessity Gap respectively. **(iv)** We conduct extensive comparisons with existing methods on six long-video benchmarks and systematic ablations of PARA-GRPO’s key design choices, demonstrating the effectiveness of ParaVT.

2 Related Work

RL for Long-Video Understanding. Long-video understanding with RL-post-trained LMMs spans three branches: (i) *tool-free RL* [7, 16, 33, 34, 37, 46] optimizes `<think>/<answer>` reasoning without tool calls; (ii) *multi-agent RL* [2, 17] jointly optimizes cooperating policy agents; (iii) our branch, *single-LMM tool-augmented RL*, where one policy emits structured tool calls inline with reasoning during rollouts: LongVT [41] (sequential `crop_video` calls), Zoom-Zero [28] (a single coarse-to-fine zoom-in pass), Conan [21] (an identify-reason-act loop over frames), VideoZoomer [6] (iterative `<video_zoom>` calls), LoVe-R1 [9] (step-decoupled iterative zoom-in), SAGE [15] (a JSON tool-action schema), and Video-o3 [45] (multi-hop clue seeking). ParaVT differs on two axes: (1) we present, to our knowledge, the first parallel single-turn multi-tool dispatch recipe for open-source Video-LMMs, compressing multiple serial context expansions into one and preserving visual-token density; (2) we identify and address the Tool Prior Paradox, an RL training failure mode specific to tool-native LMMs that prior work has not framed or addressed.

Format Stability and Tool Use in RL. In agentic RL, format stability is a precondition for tool-use learning: only parseable rollouts can be credited for their tool calls. The shallow-alignment intuition [23, 52] argues that supervised post-training is concentrated in the first few output tokens, though this hypothesis remains contested [26]. Our Format Fragility is analogous but specific to tool-native LMMs at RL-time temperature sampling: the SFT-learned `<tool_call>` tag reverts to the pretrained `<tool_code>` tag under RL rollouts, fragmenting the structural-boundary distribution. A complementary line tackles the same SFT-to-RL distributional drift before RL begins by inserting an on-policy distillation stage between SFT and RLVR with a Mixture-of-Experts discriminator that supplies perception and reasoning feedback [35]; ParaVT instead intervenes during RL itself, leaving the SFT-to-RL handoff unchanged. At the token level, RL-induced policy shifts concentrate on a sparse subset of high-divergence tokens [20]. Format tokens fall outside this class and are not preferentially updated, which explains why content accuracy improves while format degrades. To encourage exploration on tokens that drive correct outcomes, prior work relaxes the Kullback-Leibler penalty on those tokens [32]. Our Exploration Anchoring inverts both choices: it acts on the

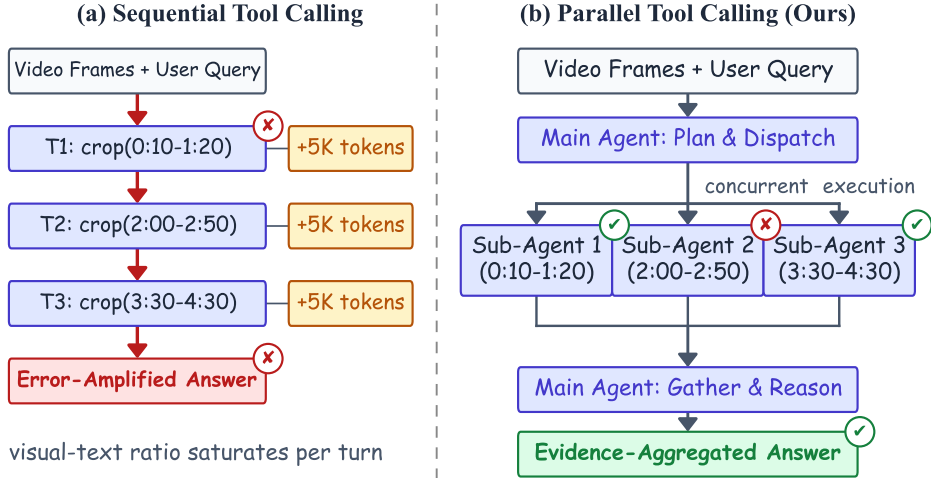


Figure 3: **Framework Comparison.** (a) *Sequential Tool Calling*: successive turns re-include the full context, accumulating visual-token overhead; a single mis-localized crop (✗) propagates errors with no peer to correct, yielding an error-amplified answer. (b) *Parallel Tool Calling (Ours)*: one main agent dispatches K tool calls concurrently to K independent sub-agents (shown for $K=3$); mis-localized peers (✗) are outvoted by correct ones (✓), yielding an evidence-aggregated answer.

complementary class of structural-boundary tokens, and adds reinforcement rather than relaxing the penalty. Our work also extends the agentic-LLM tool-use literature [24, 27, 30, 39, 40, 42] to the video setting, where visual tokens dominate the rollout context and context preservation, rather than token efficiency, becomes the primary design constraint.

3 Method

3.1 ParaVT: Parallel Video Tool Calling for Long-Video Understanding

ParaVT consists of three design elements: a parallel-dispatch architecture (Section 3.1.1), a two-stage training pipeline (Section 3.1.2), and a self-curated multi-task dataset (Section 3.1.3).

3.1.1 Framework Design

A common paradigm for tool-augmented long-video understanding lets the LMM decide *when* and *where* in the video to look more closely by issuing a `crop_video(start, end)` function call that returns the requested temporal segment with densely resampled frames for further inspection (Figure 3a). Existing realizations of this design [6, 21, 41, 47] dispatch crops *sequentially*: one tool call per turn, with the returned frames re-injected into the running context before the next turn begins.

ParaVT re-organizes the same loop as a single-turn divide-and-conquer step (Figure 3b). Within a single turn, the main agent emits K *parallel* `<tool_call>` invocations on disjoint temporal windows, each dispatched to one of K independent sub-agents that share weights with the main agent. Each sub-agent grounds only its assigned window, samples a short crop, and returns a textual summary rather than resampled frames. The gathered summaries are concatenated into a single `<tool_response>` block on which the main agent reasons to generate the final `<answer>`.

This single-turn parallel dispatch yields three concrete advantages over the sequential paradigm. (i) *Peer-Correctable Evidence*. The main agent receives K cross-checkable summaries grounded in disjoint windows by independent sub-agents, so a mis-localized window is outvoted by its peers rather than propagated down a serial chain. (ii) *Controlled Context Growth*. Returning text summaries adds only a small constant extension to the running context, while returning original frames would re-inflate it with K visual-token blocks per turn. (iii) *Bounded Inference Latency*. The K sub-agents

run concurrently, so the tool-using portion of the rollout is bounded by the slowest sub-agent rather than by their sum; dispatching more tool calls therefore does not inflate per-rollout latency.

3.1.2 Training Strategy

Cold-Start SFT with Parallel Tool Traces. The base LMM (*i.e.*, Qwen3-VL-8B-Instruct [1]) can emit a single `<tool_call>` block, but it cannot natively yield parallel tool calls in a single turn. Without supervised exposure to parallel traces, probe RL runs from the base checkpoint fail to produce parseable rollouts (Section D), and the GRPO advantage signal collapses before any tool-use credit can be assigned. Therefore, we conduct an SFT cold start on the base model with the parallel-tool corpus and select an early checkpoint as the RL initialization based on training-time format stability under temperature sampling. The two-stage SFT-then-RL pipeline is the canonical recipe for open multimodal-reasoning systems [13, 19, 22, 48]; ParaVT specializes it to parallel video-tool calling with the corpus described in Section 3.1.3 and the reward design in Section 3.2.

Agentic RL with Verifiable Rewards. Starting from the cold-started checkpoint, we conduct GRPO with two verifiable reward terms: an accuracy term against the ground-truth answer and a format term over the `<think>/<tool_call>/<answer>` schema. For each prompt, GRPO samples $G=8$ rollouts and updates the policy by their group-normalized advantage. Vanilla GRPO at this stage exposes the Format Fragility and Tool Necessity Gap introduced in Section 1. We address these failures with PARA-GRPO, a GRPO-style algorithm tailored for parallel tool-calling in agentic video RL, detailed in Section 3.2.

3.1.3 Data Curation

SFT Split. The SFT corpus contains 97K samples spanning four task families (full per-source breakdown in Table 3): general video QA (50K from LLaVA-Video-178K [50]), long-video reasoning chains (5K from LongVideo-Reason [4]), temporal grounding (12K Charades-STA [11] direct grounding + 6K Charades-STA-converted traces with parallel tool calls), and self-curated 22.5K parallel-tool traces. The mix preserves general video understanding while giving the model concentrated supervision on the parallel multi-tool schema; tool-using samples are 30% of the corpus, a fraction we settled on after an earlier larger mix (212K total at 14% tool) yielded weaker downstream tool-calling than this smaller, tool-richer plan (Section B).

The parallel-tool traces are drawn from three sources: 15K LongVT [41] tool-using rollouts, 5K Gemini-2.5-Flash [5] distillations of LongVT prompts, and 2.5K multi-segment grounding samples from MUSEG [18]. The first two sources emit one `crop_video` call per assistant turn with resampled video frames re-injected into the next turn’s context, a *sequential* format that does not exhibit the single-turn K -call schema we want ParaVT to learn. We traverse each sequential trace and merge adjacent crops whose target windows do not overlap and whose tool responses do not cross-reference each other (*e.g.*, “inspect 00:30–00:50” followed by “inspect 02:10–02:25” on independent visual evidence); calls that fail this independence check, such as a refinement crop conditioning on its predecessor, remain sequential. Each tool’s visual response is then replaced by a textual summary of the segment, aligning the SFT data with the RL sub-agent’s text-summary output format and keeping context length manageable when several crops appear in the same response.

RL Split. The RL corpus aggregates 4,406 samples on disjoint videos: 1,606 open-ended QA from filtered LongVT [41] RL data, 1,600 multiple-choice questions (MCQ) from the VideoR1 [7] RL pool, and 1,200 temporal video grounding (TVG) queries from the Charades-STA [11] training set. Before training begins, we apply a DAPO-style zero-gradient pre-filter [44] to remove samples whose advantage signal would be uninformative regardless of policy: open-ended prompts whose ground-truth answers exceed 15 words (effectively unreachable under the model’s typical short-answer regime) and prompts that received unanimously negative rollouts under the cold-started policy.

3.2 PARA-GRPO: Parseability-Anchored and Ratio-Gated GRPO

Format Fragility manifests in two forms: tag-level reversion (*i.e.*, the policy emitting the pretrained `<tool_code>` schema in place of `<tool_call>`) and structural-boundary collapse (*i.e.*, failure to close `</think>` and `</answer>`). Since the reversion direction is

$\langle \text{tool_call} \rangle \rightarrow \langle \text{tool_code} \rangle$, a natural alternative is to SFT directly on $\langle \text{tool_code} \rangle$ so that the prior and the SFT target agree. However, a substituted-tag probe shows that the reversion is bidirectional: RL still emits $\langle \text{tool_call} \rangle$ more often than the SFT-trained $\langle \text{tool_code} \rangle$ (Section H.3), so the pretrained tool prior cannot be avoided by tag choice. We therefore retain the native $\langle \text{tool_call} \rangle$ tag at SFT.

The remaining structural-boundary collapse and the Tool Necessity Gap are coupled but distinct: the former makes rollouts unparseable and removes the GRPO advantage signal, while the latter leaves the signal intact but offers no reward contrast between using and skipping tools, eliminating the incentive for tool adoption. PARA-GRPO pairs one component with each. *Exploration Anchoring* repairs rollout parseability at the structural-token boundaries where collapse concentrates, restoring GRPO’s signal. *nFrames Gating* randomizes the per-prompt overview-frame budget so that a controllable fraction of GRPO groups exhibits a non-trivial reward contrast between tool-calling and tool-skipping rollouts, creating the gradient that the Tool Necessity Gap otherwise eliminates. The order matters: only on parseable rollouts can the gating gradient be credited to tool-using behavior, so Exploration Anchoring must take effect before nFrames Gating can deliver value.

3.2.1 Exploration Anchoring

Structural-boundary collapse concentrates at closing tags. The model opens $\langle \text{think} \rangle$ on most rollouts but fails to close $\langle / \text{think} \rangle$ on a majority of them, and the same pattern propagates to $\langle / \text{answer} \rangle$. Exploration Anchoring repairs these specific boundaries via two cooperating mechanisms.

Constrained Generation. At the entry and exit of the response, two minimal interventions reinforce what SFT has already taught reliably. A *Think Prefix* pins the first tokens of every response to $\langle \text{think} \rangle \backslash n$, ruling out blind direct answers and tool calls without restricting what the model reasons about. A complementary *Answer Suffix* term in the format reward credits the presence of a final $\langle \text{answer} \rangle$ block even when intermediate structure is imperfect, so policies that recover into a well-formed answer are not penalized for exploration along the way.

Selective Anchoring. At the closing-tag boundaries where collapse concentrates, we add a targeted reward that fires only at the relevant token positions:

$$R_{\text{anchor}}(y) = \begin{cases} +\alpha & \text{if } \langle / \text{think} \rangle \text{ is correctly closed,} \\ +\beta & \text{if the full } \langle \text{think} \rangle \rightarrow \langle / \text{think} \rangle \rightarrow \langle \text{answer} \rangle \text{ flow is preserved,} \\ -\gamma & \text{if } \langle \text{think} \rangle \text{ is opened but never closed.} \end{cases} \quad (1)$$

The triplet (α, β, γ) and the outer scaling λ_{anchor} inside $R_{\text{fmt}} = R_{\text{base}} + \lambda_{\text{anchor}} R_{\text{anchor}}$ govern how aggressively the anchor pulls the policy toward parseability. By construction, anchoring fires only at structural-tag positions, not at the high-divergence content tokens that prior work on sparse policy-shift attribution targets [20], so it composes additively with the accuracy gradient rather than competing with it.

Constrained Generation and Selective Anchoring act on disjoint token populations: the former locks down entry and exit, the latter repairs internal boundaries; neither restricts the reasoning or tool-call content that lives between them.

3.2.2 nFrames Gating

Anchoring restores parseable rollouts, but parseability alone does not make tool use necessary. With a generous default overview budget, a rollout that calls `crop_video` and a rollout that skips the tool both reach the correct answer, and their rewards differ only in noise. GRPO normalizes within the group, so a near-zero reward gap produces a near-zero advantage between tool-calling and tool-skipping rollouts, and the gradient that should reinforce tool use does not exist on these prompts.

nFrames Gating creates the missing gap by randomizing the overview-frame budget per prompt:

$$n \sim \text{Uniform}(\{4, 8, 16, 32, 64\}), \quad (2)$$

where n is the number of overview frames seen by all $G=8$ rollouts in the GRPO group for that prompt. Reduced budgets ($n < 64$) push part of the visual evidence outside the overview, so rollouts

that recover that evidence through `crop_video` systematically out-score rollouts that try to answer from the truncated overview; the largest budget ($n=64$) preserves the easy regime in which direct answering is sufficient when warranted. Each training step therefore samples a mixture of budget-bound and budget-free prompts, so a controllable fraction of prompts exhibits a non-trivial reward contrast between tool-calling and tool-skipping rollouts, while on prompts where the full budget already suffices, the policy is free to skip tools without penalty. Setting this fraction too low leaves the gating signal too sparse for GRPO to learn from; setting it too high crowds out the easy regime and induces over-calling.

3.2.3 Reward Modeling

Let x denote a prompt (user query paired with the video input), y a rollout, and a^* the ground-truth answer. The composite reward sums three terms:

$$R(x, y) = R_{\text{acc}}(y, a^*) + \lambda_{\text{fmt}} R_{\text{fmt}}(y) + R_{\text{tool}}(y). \tag{3}$$

R_{acc} scores the rollout against the ground truth using a task-appropriate metric (exact match for MCQ, temporal IoU for grounding, token-level F1 for open-ended QA). R_{fmt} scores structural compliance and embeds the anchor reward R_{anchor} from Equation (1) (including the $-\gamma$ penalty for unclosed tags), so format stability and anchoring are optimized within a single scalar rather than as separate losses. R_{tool} adds a small parseability bonus for well-formed `<tool_call>` blocks.

4 Experiments

4.1 Implementation Details

Training. We initialize from Qwen3-VL-8B-Instruct [1] and SFT-cold-start on a 97K multi-task corpus; an early checkpoint is selected as the RL init by training-time format stability (selection details in Section B). RL is performed on a disjoint 4,406-sample set and pre-filtered to remove zero-gradient samples following DAPO [44]. We sample $G=8$ rollouts at $\tau=0.7$, anchor weight $\lambda_{\text{anchor}}=0.5$, and decode up to 16 frames per sub-agent crop. Training leverages AReaL [10] on a node of 8 NVIDIA GPUs (80 GB+ VRAM each), with 7 allocated to FSDP training and 1 to SGLang rollout serving. Full hyperparameters are listed in Table 4 of Section B.

Evaluation. We evaluate on six long-video benchmarks under a unified 64-frame adaptive protocol, reporting MCQ accuracy on VideoMME [8], LongVideoBench [38], LVBench [36], MLVU [53], and MMVU [51], and mean Intersection over Union (mIoU) on Charades-STA [11]. Table 1 groups open-source baselines by their training paradigm into three settings: *direct-answer* for instruct backbones with no native thinking pattern, *reasoning-enhanced* for models trained on the `<think>/<answer>` chains-of-thought schema, and *tool-augmented* for agentic models with native tool-call capabilities; GPT-4o and Gemini-1.5-Pro are reported as proprietary reference rows from their official numbers. We evaluate each baseline under the prompt class it was trained on, since a model elicits its strongest performance under the prompt distribution it was optimized for. We restrict our evaluation to natively post-trained single-LMM methods, excluding agent frameworks [3, 17, 43, 49] to keep the comparison fair. Since they compose a planner LLM with frozen vision sub-agents not trained jointly with the planner, their reported accuracy reflects orchestration quality on top of an independently trained backbone.

4.2 Main Results

As shown in Table 1, ParaVT outperforms all comparable open-source 7–8B baselines on six of the seven evaluation splits. ParaVT improves on its Qwen3-VL-8B base model across every split, with the largest gains concentrated on the long-video MCQ subset (+15.7% on LongVideoBench, +20.2% on LVBench, +11.5% on MLVU; an average relative gain of +7.9% across all seven splits). The most pronounced gain is on temporal grounding: ParaVT reaches 50.1 mIoU on Charades-STA, where the parallel `crop_video` dispatch turns temporal localization into a deliberate evidence-aggregation subroutine rather than a side capability of the underlying LMM. On long-video MCQ, ParaVT extends the open-source frontier on LongVideoBench (60.4) and LVBench (39.8) and reaches 62.1/69.4 on VideoMME (w/o / w/ subtitles), so the same single checkpoint leads on both sparse-evidence and

Table 1: **Performance Comparison with Existing Video-LMMs.** The best result is in **bold**; underline marks ParaVT’s value when it is not the benchmark-wise best. * marks cells withheld due to benchmark–training-data overlap. † marks an evaluation whose native tool-call schema could not be reconciled with the Charades-STA grounding-output format under our unified protocol, so the resulting outputs are not measurable with mIoU.

Model	VideoMME w/o sub	VideoMME w/ sub	LongVideo- Bench	LVBench	MLVU	MMVU	Charades-STA test
<i>Proprietary Video-LMMs: best-setting numbers from official reports (not under our unified protocol)</i>							
GPT-4o [14]	71.9	77.2	66.7	34.7	64.6	66.7	—
Gemini 1.5 Pro [31]	75.0	81.3	64.4	33.1	74.3	65.8	—
<i>Open Instruct Video-LMMs: direct-answer setting (native single-pass prompt)</i>							
Qwen2.5-VL-7B [25]	55.7	64.5	46.4	32.2	47.8	65.4	31.6
<i>Open Reasoning Video-LMMs: reasoning-enhanced setting (<think>→<answer>)</i>							
Video-R1-7B [7]	57.6	66.0	57.4	36.9	61.6	61.3	25.4
VideoChat-R1-7B [16]	50.4	58.2	49.2	23.8	58.7	65.0	31.5
VideoRFT-7B [33]	58.5	65.6	55.1	38.0	44.9	42.7	18.7
Time-R1-7B [37]	58.9	66.2	56.0	38.2	60.5	63.4	34.7
ReWatch-R1-7B [46]	58.8	65.0	53.6	38.5	60.1	59.8	20.2
Video-Thinker-7B [34]	61.9	65.3	56.0	*	65.2	64.5	29.0
<i>Open Agentic Video-LMMs: tool-augmented setting (<think>→<tool_call>→<answer>)</i>							
Qwen3-VL-8B [1]	59.9	68.4	52.2	33.1	58.3	68.0	49.3
Conan-7B [21]	55.5	62.8	54.5	38.2	59.2	64.0	25.4
LongVT-RFT-7B [41]	59.5	66.0	54.7	37.9	59.4	63.4	23.4
SAGE-7B [15]	44.1	52.4	37.4	31.8	49.7	55.7	28.9
VideoZoomer-7B [6]	45.3	48.3	39.6	22.9	46.2	61.6	†
ParaVT-8B (Ours)	62.1	69.4	60.4	39.8	<u>65.0</u>	68.6	50.1

grounding-heavy settings. The recipe also closes the open-source-to-proprietary gap on long-video reasoning: ParaVT surpasses GPT-4o [14] on LVBench (39.8 vs. 34.7) and MMVU (68.6 vs. 66.7).

4.3 Ablation Studies

Table 2: **Ablation Studies.** Each row reports mean training-time format reward f_τ at sampling temperature $\tau=0.7$ and mean training-time tool-call rate per rollout κ . The best result is in **bold**; underline marks ParaVT’s value when it is not the block-wise best. Rows shaded gray mark the full recipe. Block C compares inference-time dispatch modes on the same trained checkpoint, so f_τ and κ are identical across its rows and reported as “-”.

Setting	f_τ	κ	VideoMME w/o sub	VideoMME w/ sub	LongVideo- Bench	LVBench	MLVU	MMVU
<i>(A) Training Stage</i>								
Qwen3-VL-8B	0.03	0.45	59.9	68.4	52.2	33.1	58.3	68.0
+ SFT Cold-Start	0.13	2.50	60.7	69.0	58.0	39.1	63.7	67.7
+ SFT Cold-Start + GRPO	0.13	0.02	62.0	68.6	57.5	39.3	64.5	67.5
+ SFT Cold-Start + PARA-GRPO	0.41	0.21	62.1	69.4	60.4	39.8	65.0	68.6
<i>(B) Component Effectiveness</i>								
Qwen3-VL-8B + Cold-Start + GRPO	0.13	0.02	62.0	68.6	57.5	39.3	64.5	67.5
+ Exploration Anchoring	0.35	0.19	61.7	68.7	59.6	39.3	64.1	67.2
+ nFrames Gating	0.10	1.36	61.3	68.7	58.4	39.1	63.6	65.3
Full PARA-GRPO	0.41	0.21	62.1	69.4	60.4	39.8	65.0	68.6
PARA-GRPO – Tool Reward R_{tool}	0.33	0.04	61.9	68.5	57.2	38.7	64.3	67.4
PARA-GRPO – Penalty Term γ	0.36	0.27	61.6	69.0	58.9	38.8	64.5	67.7
<i>(C) Dispatch Mode</i>								
Sequential Tool Calling	-	-	61.4	68.8	57.7	37.5	64.1	66.7
Parallel Tool Calling	-	-	62.1	69.4	60.4	39.8	65.0	68.6

Training Stage. As shown in Block A of Table 2, the cold-started checkpoint over-uses tools ($\kappa=2.50$) by directly imitating tool-using demonstrations from SFT traces, and vanilla GRPO swings to the opposite extreme ($\kappa=0.02$) by skipping tools within 7 steps under the reward shortcut (Figure 1).

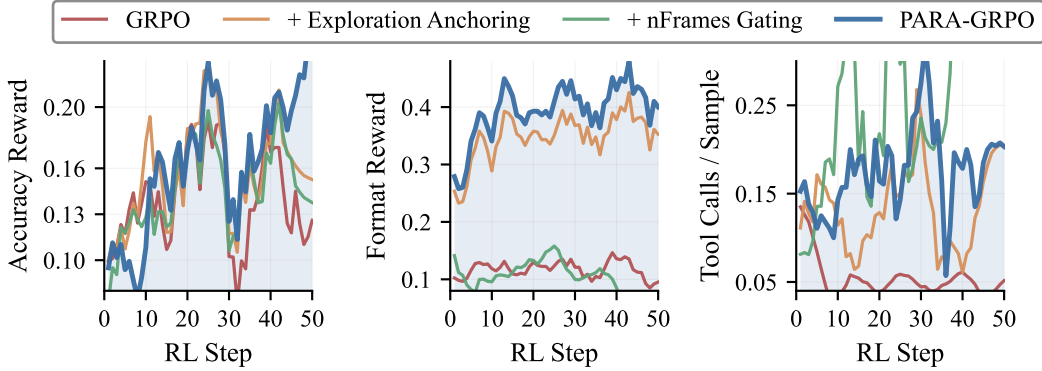


Figure 4: **Training Dynamics across PARA-GRPO Components.** Vanilla GRPO (red) stays flat at $f_\tau \approx 0.13$ while κ collapses to near zero; Exploration Anchoring (orange) lifts f_τ but keeps κ moderate; nFrames Gating (green) pushes κ off-chart while leaving f_τ low; only the full PARA-GRPO (blue) stabilizes both axes.

PARA-GRPO resolves both extremes, reaching the highest training-time mean format reward in Block A ($f_\tau=0.41$, $\kappa=0.21$), and strictly improves on vanilla GRPO across all six evaluation splits, with the largest gains on LongVideoBench and MMVU.

Component Effectiveness. Block B confirms that each PARA-GRPO component is effective. *Exploration Anchoring* alone lifts f_τ to 0.35 but leaves κ at 0.19, while *nFrames Gating* alone pushes κ to 1.36 but leaves f_τ stuck at 0.10. Only the full recipe combines parseability with tool-using incentives, reaching $(f_\tau, \kappa)=(0.41, 0.21)$ and outperforming every per-component variant on all six evaluation splits. The two ablated reward terms are each necessary: removing R_{tool} collapses tool exploration (κ falls from 0.21 to 0.04) and also drops f_τ from 0.41 to 0.33; removing the unclosed-tag penalty γ drops f_τ from 0.41 to 0.36 as the policy stops closing `</think>` reliably, costing up to 1.5 pt on LongVideoBench.

Training Dynamics. Figure 4 visualizes the same variant comparison during RL. Vanilla GRPO never recovers either metric: f_τ stays flat near 0.13 and κ collapses to near zero within 7 steps, leaving the policy in the format-shortcut regime as introduced in Section 1. *Exploration Anchoring* alone restores format ($f_\tau \rightarrow 0.35$) while keeping tool use moderate ($\kappa=0.19$). *nFrames Gating* alone pushes tool calls aggressively (κ off-chart toward 1.36) but leaves format stuck near 0.10. Only the full recipe stabilizes both axes, with f_τ rising past step 45 to a peak (0.64) that neither single component attains and κ holding moderate at 0.21.

Dispatch Mode. Block C isolates the inference-time paradigm from the policy by changing only the dispatch mode on the same trained checkpoint. Parallel dispatch outperforms sequential on every tested benchmark, with the largest gains on LongVideoBench and LVBench. Combined with the inference-cost argument in Section 3.1.1, this isolates parallel dispatch as an inference-time choice that improves accuracy without retraining.

5 Conclusion

In this work, we present **ParaVT**, the first multi-agent end-to-end RL-trained framework that enables tool-native LMMs to dispatch **Parallel Video Tool** calls in a single turn for long-video reasoning, replacing brittle sequential tool chains with peer-correctable evidence aggregation while keeping inference cost flat as the number of dispatched tools grows. By identifying the central training trade-off as the *Tool Prior Paradox* (the dual role of pretrained tool priors in driving both tool exploration and structural-format collapse under temperature sampling), we propose PARA-GRPO, which augments standard GRPO with a parseability-anchored format reward applied only at the structural-token positions most prone to collapse, and a ratio-gated frame-budget randomization that credits tools only on prompts where they are genuinely necessary. Supported by a self-curated

97K-sample multi-task SFT corpus and a separate 4,406-sample RL split spanning open-ended QA, multiple-choice, and temporal grounding, ParaVT outperforms existing open-source 7–8B baselines on six of seven long-video evaluation splits, demonstrating that anchoring format and gating tool incentives is a transferable recipe for agentic RL as tool capabilities become increasingly internalized in modern base LMMs.

References

- [1] Shuai Bai, Yuxuan Cai, Ruizhe Chen, Keqin Chen, Xionghui Chen, Zesen Cheng, Lianghao Deng, Wei Ding, Chang Gao, Chunjiang Ge, et al. Qwen3-vl technical report. *arXiv preprint arXiv:2511.21631*, 2025.
- [2] Boyu Chen, Zikang Wang, Zhengrong Yue, Kainan Yan, Chenyun Yu, Yi Huang, Zijun Liu, Yafei Wen, Xiaoxin Chen, Yang Liu, et al. Videochat-m1: Collaborative policy planning for video understanding via multi-agent reinforcement learning. *arXiv preprint arXiv:2511.19524*, 2025.
- [3] Boyu Chen, Zhengrong Yue, Siran Chen, Zikang Wang, Yang Liu, Peng Li, and Yali Wang. Lvagent: Long video understanding by multi-round dynamical collaboration of mllm agents. In *Proceedings of the IEEE/CVF International Conference on Computer Vision*, pages 20237–20246, 2025.
- [4] Yukang Chen, Wei Huang, Baifeng Shi, Qinghao Hu, Hanrong Ye, Ligeng Zhu, Zhijian Liu, Pavlo Molchanov, Jan Kautz, Xiaojuan Qi, et al. Scaling rl to long videos. *arXiv preprint arXiv:2507.07966*, 2025.
- [5] Gheorghe Comanici, Eric Bieber, Mike Schaekermann, Ice Pasupat, Noveen Sachdeva, Inderjit Dhillon, Marcel Blistein, Ori Ram, Dan Zhang, Evan Rosen, et al. Gemini 2.5: Pushing the frontier with advanced reasoning, multimodality, long context, and next generation agentic capabilities. *arXiv preprint arXiv:2507.06261*, 2025.
- [6] Yang Ding, Yizhen Zhang, Xin Lai, Ruihang Chu, and Yujiu Yang. Videozoomer: Reinforcement-learned temporal focusing for long video reasoning. *arXiv preprint arXiv:2512.22315*, 2025.
- [7] Kaituo Feng, Kaixiong Gong, Bohao Li, Zonghao Guo, Yibing Wang, Tianshuo Peng, Junfei Wu, Xiaoying Zhang, Benyou Wang, and Xiangyu Yue. Video-r1: Reinforcing video reasoning in mllms. *arXiv preprint arXiv:2503.21776*, 2025.
- [8] Chaoyou Fu, Yuhan Dai, Yongdong Luo, Lei Li, Shuhuai Ren, Renrui Zhang, Zihan Wang, Chenyu Zhou, Yunhang Shen, Mengdan Zhang, et al. Video-mme: The first-ever comprehensive evaluation benchmark of multi-modal llms in video analysis. In *Proceedings of the IEEE/CVF conference on computer vision and pattern recognition*, pages 24108–24118, 2025.
- [9] Shenghao Fu, Qize Yang, Yuan-Ming Li, Xihan Wei, Xiaohua Xie, and Wei-Shi Zheng. Love-r1: Advancing long video understanding with an adaptive zoom-in mechanism via multi-step reasoning. *arXiv preprint arXiv:2509.24786*, 2025.
- [10] Wei Fu, Jiaxuan Gao, Xujie Shen, Chen Zhu, Zhiyu Mei, Chuyi He, Shusheng Xu, Guo Wei, Jun Mei, Jiashu Wang, et al. Areal: A large-scale asynchronous reinforcement learning system for language reasoning. *arXiv preprint arXiv:2505.24298*, 2025.
- [11] Jiyang Gao, Chen Sun, Zhenheng Yang, and Ram Nevatia. Tall: Temporal activity localization via language query. In *Proceedings of the IEEE international conference on computer vision*, pages 5267–5275, 2017.
- [12] Daya Guo, Dejian Yang, Haowei Zhang, Junxiao Song, Peiyi Wang, Qihao Zhu, Runxin Xu, Ruoyu Zhang, Shirong Ma, Xiao Bi, et al. Deepseek-r1: Incentivizing reasoning capability in llms via reinforcement learning. *arXiv preprint arXiv:2501.12948*, 2025.
- [13] Wenxuan Huang, Bohan Jia, Zijie Zhai, Shaosheng Cao, Zheyu Ye, Fei Zhao, Zhe Xu, Xu Tang, Yao Hu, and Shaohui Lin. Vision-r1: Incentivizing reasoning capability in multimodal large language models. *arXiv preprint arXiv:2503.06749*, 2025.

-
- [14] Aaron Hurst, Adam Lerer, Adam P Goucher, Adam Perelman, Aditya Ramesh, Aidan Clark, AJ Ostrow, Akila Welihinda, Alan Hayes, Alec Radford, et al. Gpt-4o system card. *arXiv preprint arXiv:2410.21276*, 2024.
- [15] Jitesh Jain, Jialuo Li, Zixian Ma, Jieyu Zhang, Chris Dongjoo Kim, Sangho Lee, Rohun Tripathi, Tanmay Gupta, Christopher Clark, and Humphrey Shi. Sage: Training smart any-horizon agents for long video reasoning with reinforcement learning. *arXiv preprint arXiv:2512.13874*, 2025.
- [16] Xinhao Li, Ziang Yan, Desen Meng, Lu Dong, Xiangyu Zeng, Yinan He, Yali Wang, Yu Qiao, Yi Wang, and Limin Wang. Videochat-r1: Enhancing spatio-temporal perception via reinforcement fine-tuning. *arXiv preprint arXiv:2504.06958*, 2025.
- [17] Runtao Liu, Ziyi Liu, Jiaqi Tang, Yue Ma, Renjie Pi, Jipeng Zhang, and Qifeng Chen. Longvideoagent: Multi-agent reasoning with long videos. *arXiv preprint arXiv:2512.20618*, 2025.
- [18] Fuwen Luo, Shengfeng Lou, Chi Chen, Ziyue Wang, Chenliang Li, Weizhou Shen, Jiyue Guo, Peng Li, Ming Yan, Ji Zhang, et al. Museg: Reinforcing video temporal understanding via timestamp-aware multi-segment grounding. *arXiv preprint arXiv:2505.20715*, 2025.
- [19] Fanqing Meng, Lingxiao Du, Zongkai Liu, Zhixiang Zhou, Quanfeng Lu, Daocheng Fu, Tiancheng Han, Botian Shi, Wenhai Wang, Junjun He, et al. Mm-eureka: Exploring the frontiers of multimodal reasoning with rule-based reinforcement learning. *arXiv preprint arXiv:2503.07365*, 2025.
- [20] Haoming Meng, Kexin Huang, Shaohang Wei, Chiyu Ma, Shuo Yang, Xue Wang, Guoyin Wang, Bolin Ding, and Jingren Zhou. Sparse but critical: A token-level analysis of distributional shifts in rlvr fine-tuning of llms. *arXiv preprint arXiv:2603.22446*, 2026.
- [21] Kun Ouyang, Yuanxin Liu, Linli Yao, Yishuo Cai, Hao Zhou, Jie Zhou, Fandong Meng, and Xu Sun. Conan: Progressive learning to reason like a detective over multi-scale visual evidence. *arXiv preprint arXiv:2510.20470*, 2025.
- [22] Yingzhe Peng, Gongrui Zhang, Miaosen Zhang, Zhiyuan You, Jie Liu, Qipeng Zhu, Kai Yang, Xingzhong Xu, Xin Geng, and Xu Yang. Lmm-r1: Empowering 3b llms with strong reasoning abilities through two-stage rule-based rl. *arXiv preprint arXiv:2503.07536*, 2025.
- [23] Xiangyu Qi, Ashwinee Panda, Kaifeng Lyu, Xiao Ma, Subhrajit Roy, Ahmad Beirami, Prateek Mittal, and Peter Henderson. Safety alignment should be made more than just a few tokens deep. *arXiv preprint arXiv:2406.05946*, 2024.
- [24] Cheng Qian, Emre Can Acikgoz, Qi He, Hongru Wang, Xiusi Chen, Dilek Hakkani-Tür, Gokhan Tur, and Heng Ji. Toolrl: Reward is all tool learning needs. *arXiv preprint arXiv:2504.13958*, 2025.
- [25] Qwen Team. Qwen2.5-VL technical report. *arXiv preprint arXiv:2502.13923*, 2025.
- [26] Mohit Raghavendra, Vaskar Nath, and Sean Hendryx. Revisiting the superficial alignment hypothesis. *arXiv preprint arXiv:2410.03717*, 2024.
- [27] Timo Schick, Jane Dwivedi-Yu, Roberto Dessì, Roberta Raileanu, Maria Lomeli, Eric Hambro, Luke Zettlemoyer, Nicola Cancedda, and Thomas Scialom. Toolformer: Language models can teach themselves to use tools. *Advances in neural information processing systems*, 36: 68539–68551, 2023.
- [28] Xiaoqian Shen, Min-Hung Chen, Yu-Chiang Frank Wang, Mohamed Elhoseiny, and Ryo Hachiuma. Zoom-zero: Reinforced coarse-to-fine video understanding via temporal zoom-in. *arXiv preprint arXiv:2512.14273*, 2025.
- [29] Joar Skalse, Nikolaus Howe, Dmitrii Krasheninnikov, and David Krueger. Defining and characterizing reward gaming. *Advances in Neural Information Processing Systems*, 35:9460–9471, 2022.

-
- [30] Jianghao Su, Xia Zeng, Luhui Liu, Chao Luo, Ye Chen, and Zhuoran Zhuang. Enhancing agentic rl with progressive reward shaping and value-based sampling policy optimization. *arXiv preprint arXiv:2512.07478*, 2025.
- [31] Gemini Team, Petko Georgiev, Ving Ian Lei, Ryan Burnell, Libin Bai, Anmol Gulati, Garrett Tanzer, Damien Vincent, Zhufeng Pan, Shibo Wang, et al. Gemini 1.5: Unlocking multimodal understanding across millions of tokens of context. *arXiv preprint arXiv:2403.05530*, 2024.
- [32] Jean Vassoyan, Nathanaël Beau, and Roman Plaud. Ignore the kl penalty! boosting exploration on critical tokens to enhance rl fine-tuning. In *Findings of the Association for Computational Linguistics: NAACL 2025*, pages 6108–6118, 2025.
- [33] Qi Wang, Yanrui Yu, Ye Yuan, Rui Mao, and Tianfei Zhou. Videorft: Incentivizing video reasoning capability in mllms via reinforced fine-tuning. *arXiv preprint arXiv:2505.12434*, 2025.
- [34] Shijian Wang, Jiarui Jin, Xingjian Wang, Linxin Song, Runhao Fu, Hecheng Wang, Zongyuan Ge, Yuan Lu, and Xuelian Cheng. Video-thinker: Sparking “thinking with videos” via reinforcement learning. *arXiv preprint arXiv:2510.23473*, 2025.
- [35] Sudong Wang, Weiquan Huang, Xiaomin Yu, Zuhao Yang, Hehai Lin, Keming Wu, Chaojun Xiao, Chen Chen, Wenxuan Wang, Beier Zhu, Yunjian Zhang, and Chengwei Qin. Beyond SFT-to-RL: Pre-alignment via black-box on-policy distillation for multimodal RL. *arXiv preprint arXiv:2604.28123*, 2026.
- [36] Weihang Wang, Zehai He, Wenyi Hong, Yean Cheng, Xiaohan Zhang, Ji Qi, Ming Ding, Xiaotao Gu, Shiyu Huang, Bin Xu, et al. Lvbench: An extreme long video understanding benchmark. In *Proceedings of the IEEE/CVF International Conference on Computer Vision*, pages 22958–22967, 2025.
- [37] Ye Wang, Ziheng Wang, Boshen Xu, Yang Du, Kejun Lin, Zihan Xiao, Zihao Yue, Jianzhong Ju, Liang Zhang, Dingyi Yang, et al. Time-rl: Post-training large vision language model for temporal video grounding. *arXiv preprint arXiv:2503.13377*, 2025.
- [38] Haoning Wu, Dongxu Li, Bei Chen, and Junnan Li. Longvideobench: A benchmark for long-context interleaved video-language understanding. *Advances in Neural Information Processing Systems*, 37:28828–28857, 2024.
- [39] Zhongyu Yang, Zuhao Yang, Shuo Zhan, Tan Yue, Wei Pang, and Yingfang Yuan. Svagent: Storyline-guided long video understanding via cross-modal multi-agent collaboration. *arXiv preprint arXiv:2604.05079*, 2026.
- [40] Zhongyu Yang, Yingfang Yuan, Xuanming Jiang, Baoyi An, and Wei Pang. Inex: Hallucination mitigation via introspection and cross-modal multi-agent collaboration. In *Proceedings of the AAAI Conference on Artificial Intelligence*, volume 40, pages 29829–29837, 2026.
- [41] Zuhao Yang, Sudong Wang, Kaichen Zhang, Keming Wu, Sicong Leng, Yifan Zhang, Bo Li, Chengwei Qin, Shijian Lu, Xingxuan Li, et al. Longvt: Incentivizing “thinking with long videos” via native tool calling. *arXiv preprint arXiv:2511.20785*, 2025.
- [42] Shunyu Yao, Jeffrey Zhao, Dian Yu, Nan Du, Izhak Shafran, Karthik Narasimhan, and Yuan Cao. React: Synergizing reasoning and acting in language models. *arXiv preprint arXiv:2210.03629*, 2022.
- [43] Jinhui Ye, Zihan Wang, Haosen Sun, Keshigeyan Chandrasegaran, Zane Durante, Cristobal Eyzaguirre, Yonatan Bisk, Juan Carlos Niebles, Ehsan Adeli, Li Fei-Fei, et al. Re-thinking temporal search for long-form video understanding. In *Proceedings of the IEEE/CVF Conference on Computer Vision and Pattern Recognition*, pages 8579–8591, 2025.
- [44] Qiyang Yu, Zheng Zhang, Ruofei Zhu, Yufeng Yuan, Xiaochen Zuo, Yu Yue, Weinan Dai, Tiantian Fan, Gaohong Liu, Lingjun Liu, et al. Dapo: An open-source llm reinforcement learning system at scale. *arXiv preprint arXiv:2503.14476*, 2025.

-
- [45] Xiangyu Zeng, Zhiqiu Zhang, Yuhan Zhu, Xinhao Li, Zikang Wang, Changlian Ma, Qingyu Zhang, Zizheng Huang, Kun Ouyang, Tianxiang Jiang, et al. Video-o3: Native interleaved clue seeking for long video multi-hop reasoning. *arXiv preprint arXiv:2601.23224*, 2026.
- [46] Congzhi Zhang, Zhibin Wang, Yinchao Ma, Jiawei Peng, Yihan Wang, Qiang Zhou, Jun Song, and Bo Zheng. Rewatch-r1: Boosting complex video reasoning in large vision-language models through agentic data synthesis. *arXiv preprint arXiv:2509.23652*, 2025.
- [47] Haoji Zhang, Xin Gu, Jiawen Li, Chixiang Ma, Sule Bai, Chubin Zhang, Bowen Zhang, Zhichao Zhou, Dongliang He, and Yansong Tang. Thinking with videos: Multimodal tool-augmented reinforcement learning for long video reasoning. *arXiv preprint arXiv:2508.04416*, 2025.
- [48] Kaichen Zhang, Keming Wu, Zuhao Yang, Bo Li, Kairui Hu, Bin Wang, Ziwei Liu, Xingxuan Li, and Lidong Bing. Openmmreasoner: Pushing the frontiers for multimodal reasoning with an open and general recipe. *arXiv preprint arXiv:2511.16334*, 2025.
- [49] Xiaoyi Zhang, Zhaoyang Jia, Zongyu Guo, Jiahao Li, Bin Li, Houqiang Li, and Yan Lu. Deep video discovery: Agentic search with tool use for long-form video understanding. *arXiv preprint arXiv:2505.18079*, 2025.
- [50] Yuanhan Zhang, Jinming Wu, Wei Li, Bo Li, Zejun Ma, Ziwei Liu, and Chunyuan Li. Llava-video: Video instruction tuning with synthetic data. *arXiv preprint arXiv:2410.02713*, 2024.
- [51] Yilun Zhao, Haowei Zhang, Lujing Xie, Tongyan Hu, Guo Gan, Yitao Long, Zhiyuan Hu, Weiyuan Chen, Chuhan Li, Zhijian Xu, et al. Mmvu: Measuring expert-level multi-discipline video understanding. In *Proceedings of the Computer Vision and Pattern Recognition Conference*, pages 8475–8489, 2025.
- [52] Chunting Zhou, Pengfei Liu, Puxin Xu, Srinivasan Iyer, Jiao Sun, Yuning Mao, Xuezhe Ma, Avia Efrat, Ping Yu, Lili Yu, et al. Lima: Less is more for alignment. *Advances in Neural Information Processing Systems*, 36:55006–55021, 2023.
- [53] Junjie Zhou, Yan Shu, Bo Zhao, Boya Wu, Zhengyang Liang, Shitao Xiao, Minghao Qin, Xi Yang, Yongping Xiong, Bo Zhang, et al. Mlvu: Benchmarking multi-task long video understanding. In *Proceedings of the IEEE/CVF Conference on Computer Vision and Pattern Recognition*, pages 13691–13701, 2025.

Appendix

- **Limitations and Broader Impact** (Section A): scope limits and dual-use considerations.
- **Implementation Details** (Section B): hardware, SFT data composition and curation pipeline (sequential→parallel conversion, Gemini-CoT distillation, format/storage), RL data and DAPO zero-gradient filtering, optimizer and reward coefficients, and token-budget accounting.
- **Prompts and Templates** (Section C): verbatim system prompts used at SFT, RL, and evaluation, including the per-baseline-class evaluation prompt classes.
- **Rollout Examples** (Section D): three representative trajectories illustrating format collapse and its mitigation under PARA-GRPO.
- **Training Dynamics** (Section E): end-to-end eval progression (Figure 5) and the format↔eval correlation analysis (Figure 6).
- **Cross-Model Evidence** (Section F): per-tag format closure breakdown (Table 5) and the two-model before/after trajectory (Figure 7), extending Figure 2.
- **Tool Usage Patterns** (Section G): training-time tool-call trajectories under three reward configurations (Figure 8).
- **Negative Results** (Section H): grouped by intervention axis: reward-shape (phase-reward staging, task-aware reward coefficients), data-shape (Pre-RFT, stronger cold-start), and gradient/format-shape (Token-Decoupled GRPO structural mask, bidirectional tag reversion).

A Limitations, Broader Impact, and Future Work

Limitations. (i) The RL stage delivers its primary contribution as deployment-time format and tool-use stability under temperature sampling rather than as a large standalone greedy-eval delta on top of the cold-started checkpoint; further amplifying the eval-time translation is an open direction. (ii) The cross-model evidence for the role of the prior comes from a single Qwen2.5-VL vs. Qwen3-VL contrast (consistent with a causal interpretation but not equivalent to a controlled intervention), and the full PARA-GRPO pipeline has only been validated on Qwen3-VL-8B; extending to other tool-native LMM families and a broader pretraining-prior sweep is future work. (iii) Only the `crop_video` tool is evaluated; whether the recipe generalizes to other tool families (text retrieval, scene-graph extraction, audio transcription) is open.

Broader Impact. Agentic long-video understanding lowers the human cost of searching extended footage by content, with applications in accessibility, sports analytics, and archival retrieval. The same capability also reduces the marginal cost of large-scale surveillance over CCTV or body-camera streams, and ParaVT’s parallel-tool dispatch amplifies that throughput rather than restraining it; deployment in such contexts should be paired with explicit consent and transparency frameworks. The PARA-GRPO training recipe is tool-agnostic and could be retargeted to tool families with different safety profiles (*e.g.*, document or person retrieval), so the dual-use surface is broader than the `crop_video` tool we evaluate. We release code, data, and weights to enable independent audit but withhold surveillance-specific finetunes; downstream users adapting PARA-GRPO to higher-risk tool families should conduct their own impact assessment.

Future Work. (i) Scaling PARA-GRPO to larger LMMs (32B–72B) where richer base capabilities may make RL exploration more effective. (ii) Extending necessity gating to other agentic settings where tool necessity is not guaranteed, such as retrieval-augmented generation and code execution.

B Implementation Details

Hardware. All experiments are conducted on 2 machines, each with $8 \times$ NVIDIA GPUs (≥ 80 GB VRAM each). For RL training, we use 7 GPUs for FSDP parameter updates and 1 GPU for SGLang inference serving.

Base Model. We use Qwen3-VL-8B-Instruct [1] as the base LMM. Each video is decoded at fps=1; if the resulting frame sequence exceeds 64 frames it is uniformly subsampled to 64, otherwise the full 1-fps sequence is used.

Training Infrastructure. The AReL framework pipelines rollout generation (GPU 0, SGLang) with FSDP training (GPUs 1–7). After the first step, rollout wait drops from ~ 500 s to < 2 s due to pipelining. Each training step takes approximately 50 minutes, including ~ 35 minutes for rollout and ~ 15 minutes for parameter updates. We set `SGLANG_VLM_CACHE_SIZE_MB=4096` to accommodate 64-frame video embeddings (~ 134 MB each).

SFT Configuration. SFT uses the lmms-engine framework with FSDP. We train for 1,500 steps total, with checkpoints at every 100 steps. Learning rate: 2×10^{-5} , batch size: 32, optimizer: AdamW. The cold-started (step 500) checkpoint is selected as the RL initialization based on training-time format stability under temperature sampling (Section 4.3).

SFT Data (97K samples). The SFT training set contains 97K samples from 7 sources:

Table 3: **SFT data composition.** “Tool” indicates whether the sample contains parallel `crop_video` calls.

Dataset	Samples	Tool?	Description
LLaVA-Video-178K (subsampling)	50K	No	General video QA from the VideoR1 training pool
Self-trace (LongVT rollouts)	15K	Yes	Sequential \rightarrow parallel converted tool traces
Charades-STA	12K	No	Temporal grounding (<code>[start, end]</code>)
TVG (Charades-STA)	6K	Yes	Temporal grounding with parallel tool calls
Long video reasoning	5K	No	Multi-step reasoning on 5–60 min videos
Gemini-CoT (distilled)	5K	Yes	Tool traces generated by Gemini-2.5-Flash
MUSEG (multi-segment)	2.5K	Yes	Avg 4.4 parallel <code>crop_video</code> calls/sample

Tool-Augmented Fraction. Tool-bearing samples comprise 30% of the SFT mix. This fraction was set by a Plan A vs. Plan B comparison: an earlier Plan A (212K total, 14% tool) produced weaker tool-calling behavior in downstream RL than the current Plan B (97K total, 30% tool), despite having more raw samples. We read this as evidence that the fraction of tool-bearing samples matters more than absolute count once a non-trivial volume of non-tool video QA is present, and we did not re-tune the ratio further.

Sequential \rightarrow Parallel Conversion. The selftrace, Gemini-CoT, and TVG sources start as sequential single-tool LongVT-style traces (one `<tool_call>` per assistant turn, with cropped frames re-injected into the next turn’s context). We convert each trace to a single-turn parallel format by merging consecutive *independent* tool calls into one turn. We treat two adjacent calls as independent when their target windows do not overlap and the tool responses they consumed contain no cross-reference to one another (typical case: “inspect 00:30–00:50” followed by “inspect 02:10–02:25,” both grounded in disjoint visual evidence). Calls that fail this check (for example, a follow-up crop refining the timestamps of a previous response) are kept on their own turn. We then replace each tool’s frame response with a textual summary of the segment’s visual content, drawn from the LongVT model’s existing assistant continuation that consumed those frames. The text-summary substitution serves two purposes: it aligns the SFT data with the RL sub-agent’s output format (text, not frames) and it keeps context length manageable when several crops appear in the same response. After conversion, MUSEG remains the only source with consistently many parallel calls per turn (~ 4.4 on average); other sources average close to one call per turn because most LongVT traces issued only one crop to begin with.

Gemini-CoT Distillation. The 5K Gemini-CoT subset is produced by sampling LongVT-selfQA prompts and generating sequential tool traces with Gemini-2.5-Flash, then running them through the same sequential \rightarrow parallel conversion above. Two practical issues drove additional steps. First, Gemini’s content filter refuses certain video-question pairs; for those we re-issue the prompt to Qwen3-VL-235B as a fallback distiller and accept its trace if it passes downstream validation.

Second, raw model outputs occasionally contain JSON-structural noise (unbalanced braces, prose around the tool call); we run a GPT-4o cleanup pass that re-emits each tool call as a strict JSON block and discards any sample violating `start_time < end_time` or with an empty answer field.

Format and Storage. All splits are stored as Parquet files with the `messages` column serialized as a JSON string, sidestepping Arrow’s schema requirement when individual messages have heterogeneous tool-call structure. Each sample’s chat layout is `[system, user(video+question), assistant(think+tool_call+answer)]`. Video parameters are aligned across SFT and RL: `max_pixels = 50176 (224×224)`, `fps = 1`, `max_frames = 64`.

RL Data (4,406 samples). The RL training set is disjoint from SFT and aggregates three task families: 1,606 open-ended QA from filtered LongVT-selfQA-v2 (HACS / Ego4D-NaQ source videos), 1,600 multiple-choice from the VideoR1 pool, and 1,200 temporal-grounding queries from the Charades-STA training split (the test split is held out for evaluation, and the train/test video sets are disjoint to avoid leakage). The OE pool starts from 1,668 raw samples; we apply a DAPO-style offline filter [44] that drops two zero-gradient classes before training begins: 55 prompts whose ground-truth answers exceed 15 words (effectively unreachable given the model’s typical short-answer regime, so the F1 reward stays near zero) and 7 prompts that received unanimously negative rollouts under the cold-started policy (no signal for GRPO advantage to learn from). The filter runs once and is not re-applied as the policy evolves.

RL Configuration. GRPO training uses the AReaL asynchronous RL framework with the following hyperparameters:

Table 4: **RL training hyperparameters.**

Parameter	Value
Learning rate	2×10^{-6}
Warmup	0 steps
Temperature (τ)	0.7
GRPO group size (G)	8
Batch size	7 (must divide by 7 FSDP workers)
Max new tokens	2048
KL coefficient	0.01
Clip ratio (ϵ)	0.2
Reward bias	-0.2
FORMAT_WEIGHT	1.0
ANCHOR_WEIGHT	0.5
nFrames Gating set	{4, 8, 16, 32, 64}
Anchoring α, β, γ	0.4, 0.3, 0.3
Necessity bonus	disabled (ablation: negligible effect)
Contrastive reward	disabled (ablation: hurt performance)
Phase reward staging	disabled (ablation: 160 steps, no improvement)
<i>Infrastructure</i>	
Framework	AReaL (async RL, FSDP + SGLang)
GPU allocation	1 GPU (SGLang inference) + 7 GPUs (FSDP training)
SGLang VLM cache	4096 MB (SGLANG_VLM_CACHE_SIZE_MB)
SGLang watchdog timeout	600 s
Checkpoint save frequency	every 5 steps

Reward Function Details. Instantiating Equation (3) with the released defaults ($\lambda_{\text{fmt}}=1.0$, $\lambda_{\text{anchor}}=0.5$) gives:

$$R(x, y) = R_{\text{acc}}(y, a^*) + R_{\text{fmt}}(y) + R_{\text{tool}}(y), \quad R_{\text{fmt}}(y) = R_{\text{base}}(y) + 0.5 \cdot R_{\text{anchor}}(y).$$

Under the released default (ANSWER_SUFFIX on), the base format reward R_{base} assigns partial credit: +0.2 for substantive `<think>` content (≥ 10 chars), +0.3 for `<answer>` tag, +0.2 for `</answer>` tag, +0.3 for correct think→tool ordering, and +0.1 for balanced tag pairs. The anchoring component R_{anchor} is defined in Equation (1) with $(\alpha, \beta, \gamma)=(0.4, 0.3, 0.3)$.

The answer extraction follows a 3-level fallback: (1) content within `<answer>` tags; (2) if no `<answer>` tag, content after `</think>` excluding tool calls; (3) last non-empty line. Early detection of degenerate outputs (responses containing 5+ `<|im_start|>` tokens in under 300 characters) short-circuits to zero reward.

Token-Budget Accounting: Parallel vs. Sequential. The parallel architecture’s primary advantage is asymptotic: it re-encodes the visual context $O(1)$ rather than $O(K)$ times, where K is the number of tool calls a sample requires. Under Qwen3-VL’s 256 visual tokens per frame, a 64-frame overview consumes $\approx 16.4\text{K}$ visual tokens per turn. For a sample with K tool calls, the input-token complexity is approximately

$$T_{\text{seq}}(K) \approx K \cdot (16\text{K}_{\text{visual}} + 300_{\text{sys}}) + \frac{K(K+1)}{2} \cdot 50_{\text{hist}}, \quad T_{\text{par}}(K) \approx 16\text{K}_{\text{visual}} + 300_{\text{sys}} + K \cdot 50_{\text{hist}}, \quad (4)$$

so the asymptotic upper-bound saving grows with K (at $K=2.5$, $T_{\text{seq}} \approx 41\text{K}$ vs $T_{\text{par}} \approx 16.5\text{K}$, a $\sim 60\%$ reduction).

C Prompts and Templates

We list the system prompts used at each pipeline stage; line breaks reflect the format strings used during training.

SFT cold-start system prompt (tool-augmented sources). This prompt is used for the selftrace, Gemini-CoT, TVG, and MUSEG splits, and is the same prompt applied at RL training time:

You are a video understanding agent.

```
# Workflow
1. Think inside <think>...</think> about which video
   segments contain the evidence needed to answer.
2. Call tools using <tool_call>...</tool_call> blocks.
   You may issue multiple <tool_call> blocks in one turn
   to inspect different temporal windows in parallel.
3. After receiving <tool_response>, place your final
   answer inside <answer>...</answer>.

# Format
<think>your reasoning here</think>
<tool_call>{"name": "crop_video",
           "arguments": {"video_path": "...",
                        "start_time": ...,
                        "end_time": ...}}</tool_call>
... (more <tool_call> blocks if needed) ...
[After tool responses arrive]
<answer>your final answer</answer>

# Important
- ONLY use <tool_call> with the JSON format above.
- Do NOT use <tool_code>, Python syntax, or any other
  tool format.
- Do NOT call the same temporal window twice.
```

SFT cold-start system prompt (non-tool sources). The VideoR1, Long-video-reasoning, and Charades-STA splits do not contain tool calls; they use a minimal prompt that fixes only the reasoning and answer scaffolding:

You are a helpful video understanding assistant.
 First, reason about the question inside `<think>...</think>`.
 Then provide your final answer inside `<answer>...</answer>`.

Evaluation prompts (per baseline class). We pin one prompt class per baseline so that each row in Table 1 reflects the prompt the corresponding model was trained on (Section 4.1). *Direct-answer* (Qwen2.5-VL-Instruct): the question is asked verbatim, with no system prompt and no required output schema. *Reasoning* (Video-R1, VideoRFT, VideoChat-R1, Video-Thinker, Time-R1, ReWatch-R1): the standard `<think>...</think><answer>...</answer>` prompt, identical in shape to the non-tool SFT prompt above. *Agentic* (Qwen3-VL, Conan, ParaVT): the MATPO-style tool prompt above. The remaining tool-trained baselines use their published native schemas (`<video_zoom>` for VideoZoomer [6], the Context-VLM JSON for SAGE [15], the iMCoTT suffix for LongVT-RFT [41]).

D Rollout Examples

We present three representative rollout examples to illustrate the Format Fragility phenomenon and its mitigation.

Example 1: SFT Baseline (Greedy Decoding). Under greedy decoding, the SFT model produces well-formatted output:

```
<think>The question asks about... I should examine
the segment from 01:20 to 02:30 more closely.</think>
<tool_call>crop_video("video.mp4", 80, 150)</tool_call>
<tool_call>crop_video("video.mp4", 200, 280)</tool_call>
[tool responses...]
<answer>The person picks up the cup at 01:45.</answer>
```

Example 2: Early RL (Format Collapse). Under temperature sampling ($\tau=0.7$) without PARA-GRPO, format disintegrates:

```
<think>Looking at the video, I can see...
[reasoning continues for 500+ tokens]
[no </think> closure]
<tool_code>python
# Reverts to a non-native tool prior from pretraining
crop_video("video.mp4", start=80, end=150)
</tool_code>
[no <answer> tag, output truncated]
```

Example 3: PARA-GRPO (Recovered Format). With all PARA-GRPO components active, format is preserved under sampling:

```
<think>The question requires temporal localization.
With only 8 overview frames, I need to crop specific
segments for detail.</think>
<tool_call>crop_video("video.mp4", 75, 155)</tool_call>
<tool_call>crop_video("video.mp4", 195, 285)</tool_call>
[tool responses...]
<answer>The person picks up the cup around 01:42.</answer>
```

E Training Dynamics

Figure 5 decomposes the main eval gains into SFT and RL contributions.

F Cross-Model Evidence

F.1 Per-Tag Format Closure

Table 5 reports the per-tag closure breakdown of the Format Fragility side of the paradox (Section 1). Rows are computed from raw $\tau=0.7$ training-stream rollouts, so they reflect compliance *during* RL

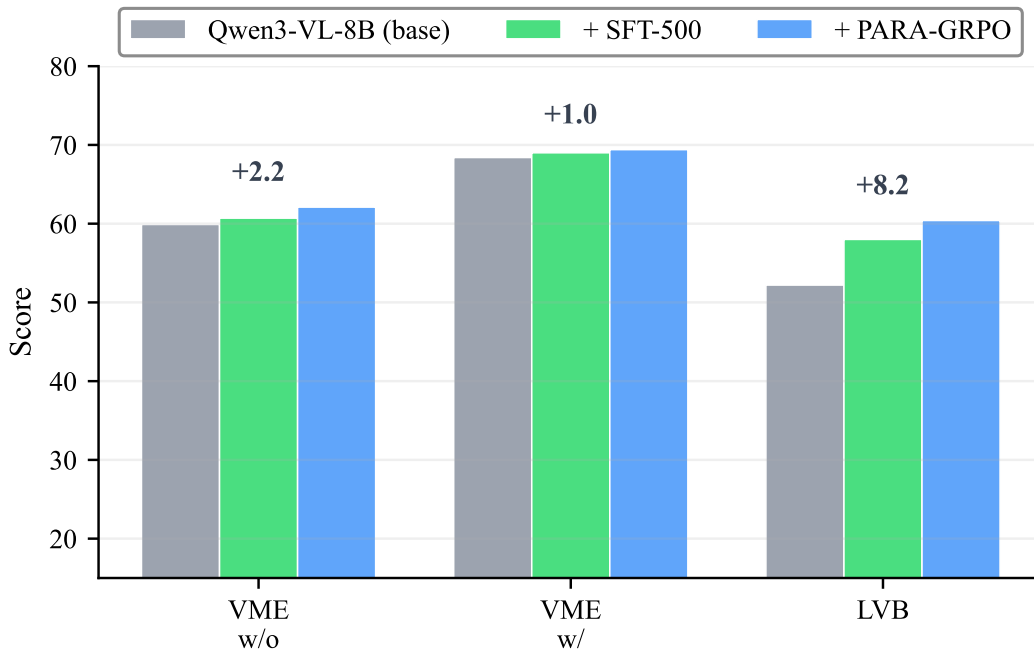


Figure 5: **End-to-end progression** from Qwen3-VL-8B through the cold-started (step 500) checkpoint to PARA-GRPO across three 64f QA-style benchmarks (VideoMME w/o sub, VideoMME w/ sub, LongVideoBench). Numbers above each triplet are the base→PARA-GRPO delta. The cold start delivers the bulk of the eval headroom, and RL adds the training-time format and tool-use stability that transfers to deployment-time robustness (Figure 4).

exploration. Vanilla GRPO halves the cold-start-learned closure rates within 9 steps as the policy reward-hacks toward direct answering; PARA-GRPO restores all three rates above the cold-started (step 500) baseline by step 19.

Table 5: **Format Fragility Quantified.** Each row reports the closure rates of the three structural tags in raw $\tau=0.7$ rollouts sampled from training streams. `<think>`: fraction of completions with a properly closed reasoning block. `<tool_call>`: fraction with a closed and JSON-parseable tool-call block, the agentic tag whose collapse most directly disables tool-augmented reasoning. `<answer>`: fraction with a properly bracketed answer block. Vanilla GRPO halves the cold-start-learned closure rates within 9 steps as the policy reward-hacks toward direct answering; PARA-GRPO restores them via Selective Anchoring at structural-boundary tokens. † marks the full PARA-GRPO recipe.

Configuration ($\tau=0.7$ rollouts)	N	<code><think></code>	<code><tool_call></code>	<code><answer></code>
Cold-start (step 500) (pre-RL baseline)	166	51.8%	47.4%	30.1%
Phase C step 9 (vanilla GRPO, no PARA-GRPO)	56	26.8%	18.2%	19.6%
Constrained only step 9 (no anchor)	56	14.3%	9.5%	10.7%
PARA-GRPO step 9 (anchor active)	56	30.4%	31.7%	28.6%
PARA-GRPO step 19 (anchor stabilized) †	56	58.9%	52.6%	41.1%

F.2 Two-Model Trajectory

Figure 2 in the main body summarizes the cross-model contrast (Qwen2.5-VL vs. Qwen3-VL) at the two endpoints of the prior gradient. Figure 7 provides the complementary before/after view of the same two checkpoints over the full 520-step training horizon.

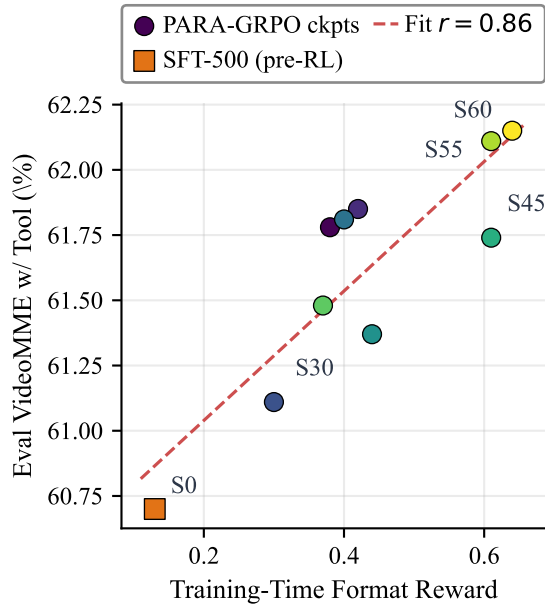


Figure 6: **Format↔eval correlation** across 10 PARA-GRPO checkpoints. Training-time format reward (x) tracks greedy-eval VideoMME accuracy (y) at Pearson $r=0.86$ ($p<0.01$); the square marks the cold-started (step 500) pre-RL anchor.

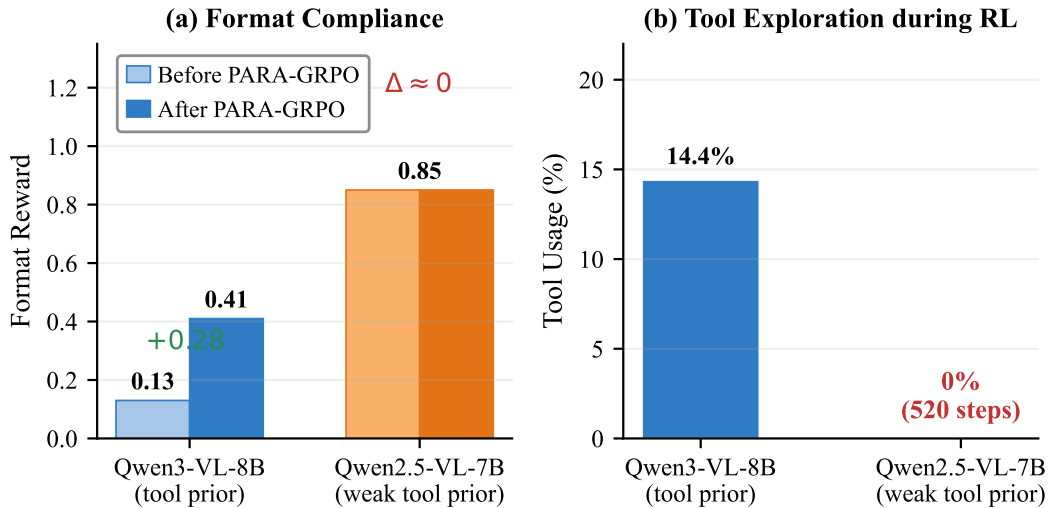


Figure 7: **The Tool Prior Paradox (two-model trajectory)**. (a) Qwen3-VL’s format climbs from 0.13 to 0.41 under PARA-GRPO; Qwen2.5-VL stays near 0.85. (b) Qwen3-VL settles at a moderate tool-call rate ($\kappa=0.21$ calls per rollout); Qwen2.5-VL emits zero tool calls. Complements Figure 2.

G Tool Usage Patterns

Figure 8 traces training-time tool-call trajectories under three reward configurations (no penalty, no-tool penalty only, full PARA-GRPO).

H Negative Results and Failure Modes

We organize the negative results by the axis they intervene on: *reward-shape* (Phase staging, Task-Aware coefficients), *data-shape* (Pre-RFT, Stronger Cold-Start), and *gradient/format-shape* (TD-

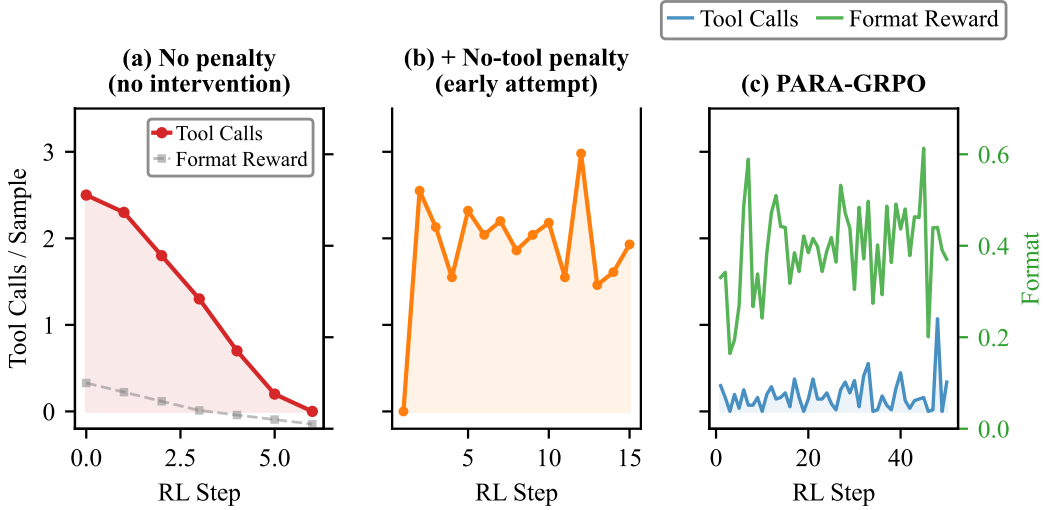


Figure 8: **Training-time tool usage** (rollout averages at $\tau=0.7$, group size 8). (a) Early GRPO without intervention: tool usage drops from 2.5 to 0 by step 7 (reward hacking). (b) A no-penalty variant keeps tool calls but format stays low. (c) Under PARA-GRPO, κ stabilizes at 0.1–0.5 while f_τ (green, right axis) climbs to 0.41.

GRPO mask, Bidirectional tag reversion). Each fails for a distinct reason that further constrains the design space.

H.1 Reward-Shape Interventions

Phase Reward Staging. We first optimized format reward in isolation, planning to introduce accuracy reward once format stabilized. After 160 steps of format-only optimization, f_τ remained at 0.13 with no upward trend, suggesting format and accuracy signals are interdependent: the model needs the accuracy gradient to motivate format learning in the first place.

Task-Aware Reward Coefficients. We added task-aware coefficients ($1.5\times$ for concise MCQ answers, $0.3\text{--}0.4\times$ for verbose ones) on top of PARA-GRPO. Training-time accuracy reward improves from 0.15 to 0.24 over 30 steps and format compliance stays comparable at 0.39, but the variant does not outperform base PARA-GRPO on held-out eval: the best checkpoint reaches VideoMME 61.81 (vs. PARA-GRPO’s 62.11) and LongVideoBench 58.26 (vs. 60.40). Task-aware shaping improves training signal quality without translating into held-out eval gains, so we keep the simpler unweighted accuracy reward in the default recipe.

H.2 Data-Shape Interventions

Pre-RFT (rejection fine-tuning). We sampled $\tau=0.7$ rollouts from the cold-started checkpoint, filtered for format-compliant samples, and mixed them back into SFT training. Subsequent RL from this Pre-RFT init peaked at $f_\tau=0.40$, but the partially-formatted samples in the SFT corpus degraded the cold-start quality on every downstream metric, ruling out the pre-RL refinement route.

Stronger Cold-Start, Worse RL. Augmenting cold-start data with 12% parallel tool-calling samples (106K vs. 97K) produces a stronger cold-started checkpoint (VideoMME 61.3 \rightarrow 62.3). RL from this stronger init produces zero tool calls throughout training. Three factors compound: (i) the stronger model answers correctly without tools even under gating, so the tool-rewarded gradient is averaged out; (ii) mixed single/parallel tool patterns in the cold-start data increase Format Fragility; (iii) more thorough SFT coverage shifts the policy toward reproducing the cold-start distribution rather than exploring. These coupled effects motivate keeping the cold-start scope to the format schema rather than expanding it into the tool-call distribution itself.

H.3 Gradient and Format-Shape Interventions

Token-Decoupled GRPO (TD-GRPO) Structural Mask. We test a token-decoupled GRPO variant that selectively zeros the policy-gradient contribution of structural tokens (e.g., `<think>`, `<tool_call>`) so that RL only updates semantic content tokens, following prior work on sparse critical-token reweighting [20]. After 11 steps, f_τ dropped to 0.11 (below baseline 0.13): zeroing gradients on format tokens tells the model format is irrelevant to reward, the opposite of what stabilizing format requires.

Bidirectional Format Reversion. Our main runs SFT with `<tool_call>`, which is Qwen3-VL’s native tool-calling tag: it is present in the tokenizer vocabulary as a single added token (ID 151657) and is the format emitted by the model’s default chat template. To probe whether Format Fragility is a mismatch between the SFT tag and the pretraining prior, we re-run SFT with `<tool_code>` instead: a four-subword sequence (`[<, tool, _code, >]`) that Qwen3-VL encountered during pretraining (e.g., through code-block tool formats in public datasets) but that is not in the tokenizer’s added vocabulary. The `<tool_code>`-trained model still generates `<tool_call>` in 5.4% of rollouts (despite never seeing it during SFT), while its trained `<tool_code>` appears in only 1.8%. This *bidirectional format reversion* (Figure 9) confirms that Format Fragility stems from mode instability across *multiple* pretrained tool representations rather than from a single mismatched tag: regardless of which tag we choose for SFT, the pretrained tool prior resurfaces at temperature sampling and fragments the output distribution. The format-substituted model also shows lower total tool emission (7.2% vs. 14.4% of rollouts emit any tool tag), consistent with the probability-mass argument that single-token special tokens are more efficiently reinforced by RL than multi-subword sequences.

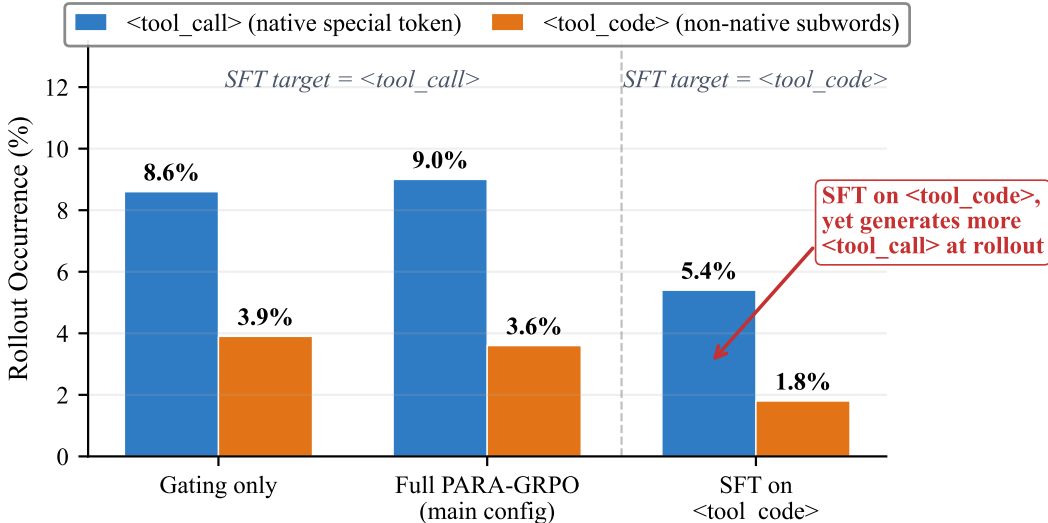


Figure 9: **Bidirectional tag reversion during RL.** SFT with `<tool_call>`: RL also emits `<tool_code>` (3.6–3.9% of rollouts). SFT with `<tool_code>`: RL still emits `<tool_call>` more often (5.4%) than the SFT-trained tag (1.8%). Tag substitution does not remove Format Fragility.